SPARSE AND CROSS-TERM FREE TIME-FREQUENCY DISTRIBUTION BASED ON HERMITE FUNCTIONS

Branka Jokanovic and Moeness Amin

Center for Advanced Communications, Villanova University, Villanova, PA 19085, USA

ABSTRACT

Hermite functions are an effective tool for improving the resolution of the single-window spectrogram. In this paper, we analyze the Hermite functions in the ambiguity domain and show that the higher order terms can introduce undesirable cross-terms in the multiwindow spectrogram. The optimal number of Hermite functions depends on the location and spread of signal auto-terms in the ambiguity domain. We apply and compare several sparsity measures, namely ℓ_1 norm, the Gini index and the time-frequency concentration measure, for determining the optimal number of Hermite functions, leading to the most desirable time-frequency representation. Among the employed measures, the Gini index provides the sparsest solution. This solution corresponds to a well-concentrated and cross-term reduced time-frequency signature.

Index Terms— Ambiguity function, cross-terms, Hermite functions, kernel, time-frequency distribution

1. INTRODUCTION

The frequency contents of a majority of biological and man made signals change in time [1]. Examples include EEG, radar signals and speech [2], [3]. In order to analyze the time-varying nature of the signal spectrum, linear and quadratic time-frequency representations (TFRs) can be used. Various time-frequency distributions have been defined, none of which provides a desirable TFR for all signal types.

The simplest linear TFR is the Short-time Fourier transform (STFT) [1]. It is obtained as the Fourier transform of the sliding window in time. Energetic version of the STFT is the spectrogram. The major drawback of the spectrogram is that its efficiency depends on the employed window size and shape. Namely, due to the uncertainty principle, one cannot design a window which is simultaneously narrow in both time and frequency domains. This creates a trade-off between spectral and temporal resolution. Improvement in resolution, however, can be achieved using multiple windows STFTs. A set of Hermite functions is known to provide excellent resolution properties of the spectrogram when compared to its single-window counterpart [4], [5]. It has been shown that these functions provide maximum signal concentration in the joint time-frequency domain with elliptic symmetry [6]. This property has motivated their use for various types of signals, including locally stationary processes and radar signals [7]-[9].

In this paper, we examine the Hermite functions in the ambiguity domain and show that they act as a low-pass kernel. The spread of this kernel would depend on the number of the employed functions. We demonstrate that the inclusion of more Hermite functions leads to a larger kernel volume, which could capture undesirable cross-terms. Thus, there is a need to determine the optimal number of Hermite functions in order to achieve good resolution property, while avoiding cross-terms. We propose an approach which determines this number based on measuring the sparsity of the time-frequency representation. Among different sparsity measures, the Gini index is shown to have the best performance.

This paper differs from past work on sparsity and quadratic TFR. It does not perform sparse reconstruction of the TFR from compressed ambiguity domain observations [10], nor does it obtain TFR by sparse reconstructions from a windowed randomly sampled data [11] or from the corresponding instantaneous autocorrelation function [12]. Rather, this paper defines a new member of Cohen's class in which the overall equivalent time-frequency kernel, derived from the Hermite functions, leads to the sparsest solution.

This paper is organized as follows. Section 2 provides a brief description of the Hermite functions and the multiwindow spectrograms. In Section 3, the multiwindow spectrogram and the corresponding set of windows are analyzed in the ambiguity domain. An approach for determining the optimal number of Hermite functions is also given in Section 3. Simulation results are provided in Section 4, while the conclusion is given in Section 5.

2. THE MULTI-WINDOW SPECTROGRAM BASED ON A SET OF HERMITE FUNCTIONS

The Hermite functions of the 0th and 1st order are defined as

$$\psi_0(t) = \frac{1}{\sqrt[4]{\pi}} e^{-t^2/2}, \tag{1}$$

$$\psi_1(t) = \frac{\sqrt{2}t}{\sqrt[4]{\pi}} e^{-t^2/2}. \quad (2)$$

The Hermite functions of higher order can be defined using the recursive relation

$$\psi_l(t) = t\sqrt{\frac{2}{l}}\psi_{l-1}(t) - \sqrt{\frac{l-1}{l}}\psi_{l-2}(t), \forall l \geq 2. \quad (3)$$

These functions are used as windows in the multi-window spectrogram $SPEC_{MW}(t,\omega)$, which can be expressed as the weighted sum of L spectrograms $SPEC_l(t,\omega)$, $l = 0, 1...L-1$, i.e. [4],

$$SPEC_{MW}(t,\omega) = \sum_{l=0}^{L-1} c_l(t) SPEC_l(t,\omega). \quad (4)$$

Each spectrogram in (4) is obtained by using a Hermite function of l-th order $\psi_l(\tau)$ as the window function, i.e.,

$$SPEC_l(t,\omega) = \left| \int_{-\infty}^{\infty} s(t+\tau)\psi_l(\tau) e^{-\jmath\omega\tau} d\tau \right|^2. \quad (5)$$

If the signal $s(t)$ is represented in terms of its amplitude and phase, i.e., $s(t) = A(t)e^{\jmath\varphi(t)}$, and if this amplitude is slowly varying within the window, then the weights $c_l(t)$ can assume constant values [4]. In this paper, we apply this property in order to simplify the analysis.

3. THE OPTIMAL NUMBER OF HERMITE FUNCTIONS FOR CROSS-TERMS SUPPRESSION

3.1. The Hermite functions in the ambiguity domain

In this section, the role of window functions in the multiwindow spectrogram is observed in the ambiguity domain. In this domain, the desirable signal components, namely auto-terms, reside in the proximity of the origin, while undesirable cross-terms appear distant from the domain axes and the origin. The spectrogram is considered as a distribution within the Cohen class, i.e.,

$$SPEC(t,\omega) = 2\pi \int_{-\infty}^{\infty}\int_{-\infty}^{\infty} A_s(\theta,\tau)\Phi(\theta,\tau) e^{-\jmath(\theta t+\omega\tau)} d\theta d\tau, \quad (6)$$

where $A_s(\theta,\tau)$ denotes the ambiguity function of signal $s(t)$, and $\Phi(\theta,\tau)$ is the kernel which, in the spectrogram case, is equal to the ambiguity function of the window $\psi(\tau)$. Most kernels assume low-pass filter characteristics consistent with the auto- and cross-terms location in the ambiguity plane. Using (6), the multiwindow spectrogram can be written as the two-dimensional Fourier transform (2DFT) of the product of the signal ambiguity function and the sum of the kernels produced by the employed set of Hermite functions,

$$SPEC_{MW}(t,\omega) = 2DFT_{\theta,\tau}[2\pi A_s(\theta,\tau)\sum_{l=1}^{L}\Phi_l(\theta,\tau)]. \quad (7)$$

Each kernel $\Phi_l(\theta,\tau)$ can be defined as the scaled ambiguity function of the l-th order Hermite window, i.e.,

$$\Phi_l(\theta,\tau) = c_l \int_{-\infty}^{\infty} \psi_l(t+\frac{\tau}{2})\psi_l^*(t-\frac{\tau}{2}) e^{-\jmath\theta t} dt. \quad (8)$$

Before providing the general expression for the kernel $\Phi_l(\theta,\tau)$, we first compute the kernels for the lowest order Hermite functions. The kernel $\Phi_0(\theta,\tau)$ is

$$\begin{aligned}\Phi_0(\theta,\tau) &= c_0 \int_{-\infty}^{\infty} \tfrac{1}{\sqrt{\pi}} e^{-\frac{t^2}{2}-\frac{\tau^2}{4}} e^{-\jmath\theta t} dt \\ &= c_0 \tfrac{1}{\sqrt{2}\sqrt{\pi}} e^{-(\frac{\theta^2}{2}+\frac{\tau^2}{4})}. \end{aligned} \quad (9)$$

In essence, using the 0-th order Hermite function corresponds to applying a kernel in the ambiguity domain which has a shape of radial Gaussian. This kernel offers its highest values when the two variables are close to zero, making it dominant around the origin. It can be readily shown that the kernel which corresponds to the 1st order Hermite function is given by

$$\begin{aligned}\Phi_1(\theta,\tau) = &\quad c_1 \int_{-\infty}^{\infty} \tfrac{2}{\sqrt{\pi}}(-(\tfrac{t^2}{2}+\tfrac{\tau^2}{4})) e^{-(\frac{t^2}{2}+\frac{\tau^2}{4})} e^{-\jmath\theta t} dt \\ &= c_1 \tfrac{\sqrt{2}}{\sqrt{\pi}}(-(\tfrac{\theta^2}{2}+\tfrac{\tau^2}{4})) e^{-(\frac{\theta^2}{2}+\frac{\tau^2}{4})} + \tfrac{c_1}{c_0}\Phi_0(\theta,\tau). \end{aligned} \quad (10)$$

If we observe the first term of the above kernel, we find that the kernel volume is larger than that of the kernel $\Phi_0(\theta,\tau)$. Hence, by employing two Hermite functions instead of one, more terms in the ambiguity domain will contribute to the formation of the signal TFR. In order to examine the effect of the higher order Hermite functions, we recall that the lth order function can be expressed as

$$\psi_l(t) = p_l(t) e^{-\frac{t^2}{2}}, \quad (11)$$

where $p_l(t)$ is a polynomial of order l. Using this representation and the fact that Hermite functions are eigenfunctions of the Fourier transform, i.e., $\psi_l(\omega) = (-\jmath)^l\psi_l(t)$, the kernel $\Phi_l(\theta,\tau)$ can be represented as

$$\begin{aligned}\Phi_l(\theta,\tau) &\approx \int_{-\infty}^{\infty} (p_{2l}(t) + p_{2l}(\tfrac{\tau}{2})) e^{-(\frac{t^2}{2}+\frac{\tau^2}{4}+\jmath\theta t)} dt + r(\theta,\tau) \\ &\approx (\tfrac{\theta^2}{2}+\tfrac{\tau^2}{4})^l e^{-(\frac{\theta^2}{2}+\frac{\tau^2}{4})} + r(\theta,\tau), \end{aligned} \quad (12)$$

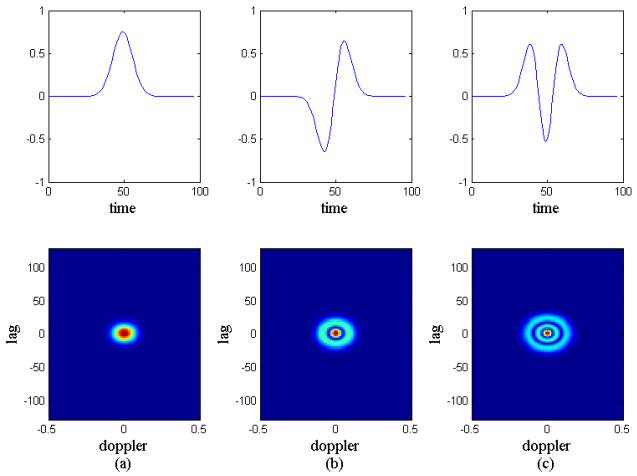

Fig. 1. Hermite functions in time and ambiguity domain: (a) 0th order, (b) 1st order, (c) 2nd order.

where $r(\theta,\tau)$ denotes contributions to the kernel from polynomials of order smaller than $2l$. Since we seek the contribution of the highest term in polynomial, we write the first term in (12) as

$$\phi^l(\theta,\tau) = e^{-(\frac{\theta^2}{2}+\frac{\tau^2}{4})(1-l\frac{\ln(\frac{\theta^2}{2}+\frac{\tau^2}{4})}{\frac{\theta^2}{2}+\frac{\tau^2}{4}})}. \quad (13)$$

By increasing l, the argument of the exponential becomes larger which increases the kernel extent and its volume. This implies that the inclusion of higher order Hermite functions is not necessary and could be counterproductive due to the capturing of the ambiguity domain cross-terms. Fig. 1 shows the Hermite functions of 0th, 1st and 2nd order and their corresponding kernels. The kernel volume increases as we increase the order of the Hermite function.

3.2. An approach for determining the optimal number of Hermite functions

In order to determine the optimal number of Hermite functions, we use sparsity measures. It can be shown that the spread of the kernel in the ambiguity domain influences sparsity of the TFR [13]. In other words, the inclusion of more cross-terms in the ambiguity domain reduces sparsity of the TFR. Using this property, we can determine the number of Hermite functions necessary to provide the sparsest solution, defined as the TFR which contains only auto-terms. The optimization problem can be formulated as follows,

$$\begin{aligned} \underset{L}{\text{minimize}} \quad & \| \mathbf{X} \|_0 \\ \text{subject to} \quad & \mathbf{X} = 2DFT[2\pi \mathbf{A_s} \odot \sum_{l=1}^{L} \mathbf{\Phi_l}], \end{aligned} \quad (14)$$

where $\| \cdot \|_0$ corresponds to ℓ_0 norm and $\mathbf{X}$ represents TFR based on multiple Hermite functions. It should be noted that vectorized forms of the TFR are used when measuring sparsity. The ℓ_0 norm measures the number of non-zero elements within a matrix $\mathbf{X}$. However, this norm is sensitive to noise which makes it unsuitable for use in practice. Other norms and measures can be defined. The most common substitute for ℓ_0 norm is ℓ_1 norm which for the real-valued signal vector $\mathbf{x}, x(1) \leq ... \leq x(N)$ is defined as

$$\| \mathbf{x} \|_1 = \sum_{n=1}^{N} | x(n) | . \quad (15)$$

In [14], the authors proposed a set of attributes which a sparsity measure should intuitively have. They compared several measures, including ℓ_1 norm, and proved that the Gini index and the pq-mean satisfy all desirable properties, rendering them good candidates for measuring sparsity. The Gini index for the sorted real-valued vector $\mathbf{x}$ can be defined as

$$GI(\mathbf{x}) = 1 - 2\sum_{n=1}^{N} \frac{x(n)}{\|x\|_1} \frac{N-n+0.5}{N}. \quad (16)$$

As the number of non-zero values of the signal decreases, the value of the Gini index increases. The pq-mean measure of the real-valued vector $\mathbf{x}$ is defined as

$$pq(\mathbf{x}) = -\frac{(\frac{1}{N}\sum_{k=1}^{N} x^p(k))^{1/p}}{(\frac{1}{N}\sum_{k=1}^{N} x^q(k))^{1/q}}. \quad (17)$$

If we use $p = 4$ and $q = 2$, and the fourth power is computed, one of the well-known TFR concentration measures emerges [15]. Even though this measure satisfies desirable properties for measuring sparsity, it has its own disadvantage. Namely, in the case of multiple signal components, this measure could favor highly localizable cross-terms in lieu of less concentrated auto-terms. In Section 4, three sparsity measures are examined, namely the Gini index, the time-frequency concentration measure [15] and ℓ_1 norm. The results suggest the use of the Gini index for measuring sparsity in the time-frequency plane.

4. SIMULATIONS

In this section, we evaluate the proposed approach using multi-component non-stationary signals. In all plots, frequency axis is normalized.

In the first example, we observe a signal in the presence of noise (SNR = 0dB) which has two sinusoidal frequency modulated (FM) components and a sinusoid, i.e.,

$$x(n) = 2e^{\jmath 16\sin(2\pi n)+\jmath 64n} + 2e^{\jmath 16\sin(2\pi n)-\jmath 96n} + 2e^{\jmath 64n}.$$

These types of signals are common in radar applications. The sinusoidal FM signal can be used to model rotating parts

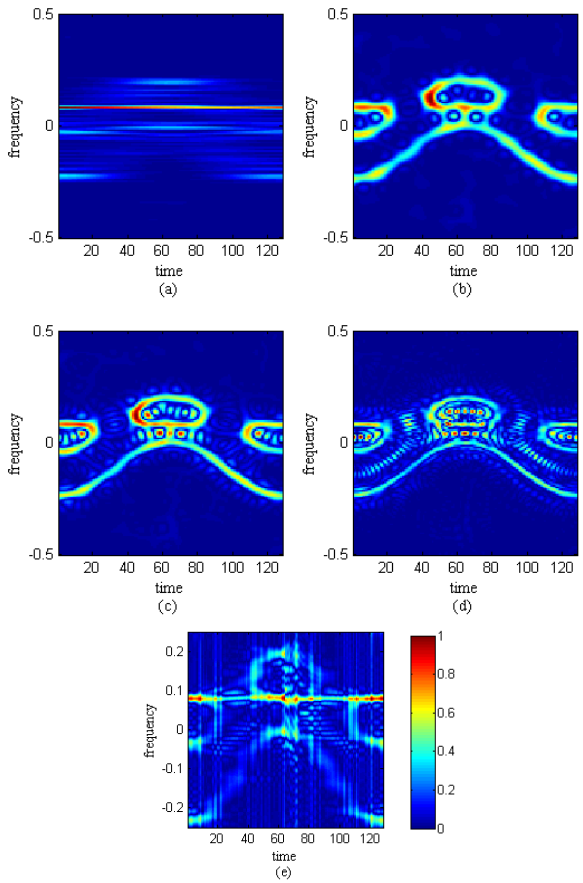

Fig. 2. Different TFRs in the presence of noise. For multiwindow TFRs, number of windows is determined by different sparsity measures: (a) Single-window spectrogram, (b) TFR based on Gini index, (c) TFR based on time-frequency concentration measure, (d) TFR based on ℓ_1 norm, (e) CWD.

of a target, while sinusoid is used to model the rigid body. Fig. 2(a) demonstrates poor resolution property of the single-window spectrogram. Choi-Williams distribution (CWD)[16] in Fig. 2(e) suppresses the cross-terms, but auto-terms are also affected. In Fig. 2 (b, c, d), multiwindow TFRs are shown based on different sparsity measures. We notice that the Gini index has significantly suppressed the cross-terms which is the result of estimating the optimal number of Hermite functions. Fig. 3 depicts how sparsity changes for different number of windows according to the observed sparsity measures. The Gini index requires the smallest number of functions and leads to the best TFR.

In the following example, we observe real-data, namely human gait. Data is obtained at the Radar Imaging Lab at Villanova University. Results are shown in Figs. 4 and 5. The multiwindow TFR based on the Gini index improves the concentration of single-window spectrogram, rendering the human gait features more prominent and simple to extract.

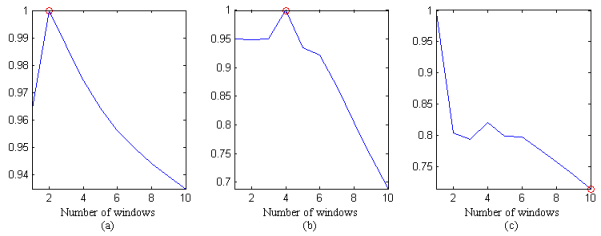

Fig. 3. The change of sparsity according to different measures: (a) Gini index, (b) Time-frequency concentration measure, (c) ℓ_1 norm. Red circle denotes the point where sparsest representation occurs according to each measure.

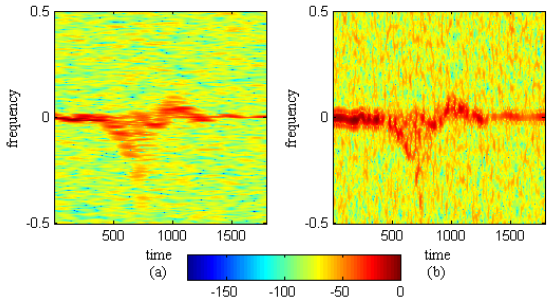

Fig. 4. TFR for data representing a human fall: (a) Single-window spectrogram, (b) The multiwindow TFR based on Gini index.

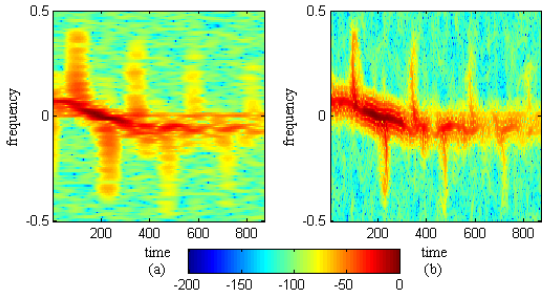

Fig. 5. TFR for data representing a person walking with one arm swinging: (a) Single-window spectrogram, (b) The multiwindow TFR based on Gini index.

5. CONCLUSION

In this paper, the behavior of the multiwindow spectrogram, based on a set of Hermite functions, is analysed in the ambiguity domain. Analysis showed that the Hermite functions form a kernel in the ambiguity plane which, in the case of lower order functions, behaves as a low-pass filter. Using more Hermite functions can improve resolution, but will result in the inclusion of undesirable cross-terms. These cross-terms compromise sparsity of the time-frequency signature and as such should be avoided. By using the Gini index as a sparsity measure, an optimum number of Hermite functions can be determined.

6. REFERENCES

[1] L. Cohen, "Time-frequency distributions-a review," *Proc. IEEE*, vol. 77, no. 7, pp. 941–981, 1989.

[2] Y. Xu, S. Haykin, and R. J. Racine, "Multiple window time-frequency distribution and coherence of EEG using Slepian sequences and Hermite functions," *IEEE Trans. Bio. Engin.*, vol. 46, no. 7, pp. 861–866, 1999.

[3] P. Setlur, M. Amin, and T. Thayaparan, "Micro-Doppler signal estimation for vibrating and rotating targets," in *Proc. 8th Int. Symp. Signal Process. and Appl.*, vol. 2, Sydney, Australia, Aug. 2005, pp. 639–642.

[4] F. Çakrak and P. J. Loughlin, "Multiwindow time-varying spectrum with instantaneous bandwidth and frequency constraints," *IEEE Trans. Signal Process.*, vol. 49, no. 8, pp. 1656–1666, 2001.

[5] G. Fraser and B. Boashash, "Multiple window spectrogram and time-frequency distributions," in *Proc. IEEE ICASSP*, vol. 4, 1994, pp. IV–293.

[6] P. Flandrin, "Maximum signal energy concentration in a time-frequency domain," in *Proc. IEEE ICASSP*, 1988, pp. 2176–2179.

[7] M. Hansson-Sandsten, "Evaluation of the optimal lengths and number of multiple windows for spectrogram estimation of SSVEP," *Medical engineering & physics*, vol. 32, no. 4, pp. 372–383, 2010.

[8] P. Wahlberg and M. Hansson, "Kernels and multiple windows for estimation of the Wigner-Ville spectrum of Gaussian locally stationary processes," *IEEE Trans. Signal Process.*, vol. 55, no. 1, pp. 73–84, 2007.

[9] I. Orovic, S. Stankovic, T. Thayaparan, and L. Stankovic, "Multiwindow S-method for instantaneous frequency estimation and its application in radar signal analysis," *IET Signal Process.*, vol. 4, no. 4, pp. 363–370, 2010.

[10] P. Flandrin and P. Borgnat, "Time-frequency energy distributions meet compressed sensing," *IEEE Trans. Signal Process.*, vol. 58, no. 6, pp. 2974–2982, 2010.

[11] M. G. Amin, B. Jokanovic, and T. Dogaru, "Reconstruction of locally frequency sparse nonstationary signals from random samples," in *Proc. Signal Process. Conf. (EUSIPCO)*, Lisbon, Portugal, Sep. 2014, pp. 1–5.

[12] Y. D. Zhang, M. G. Amin, and B. Himed, "Reduced interference time-frequency representations and sparse reconstruction of undersampled data," in *Proc. Signal Process. Conf. (EUSIPCO)*, Marrakech, Morocco, Sep. 2013, pp. 1–5.

[13] B. Jokanovic and M. Amin, "Multi-task time-frequency kernel design in the case of compressed data," *submitted to IEEE Trans. Signal Process.*, 2014.

[14] N. Hurley and S. Rickard, "Comparing measures of sparsity," *IEEE Trans. Inf. Theory*, vol. 55, no. 10, pp. 4723–4741, 2009.

[15] D. L. Jones and T. W. Parks, "A high resolution data-adaptive time-frequency representation," *IEEE Trans. Acoust. Speech Signal Process.*, vol. 38, no. 12, pp. 2127–2135, 1990.

[16] H. I. Choi and W. J. Williams, "Improved time-frequency representation of multicomponent signals using exponential kernels," *IEEE Trans. Acoust. Speech Signal Process.*, vol. 37, no. 6, pp. 862–871, Jun. 1989.